THE JOURNAL OF PHYSICAL CHEMISTRY



Subscriber access provided by OKLAHOMA STATE UNIV

B: Liquids, Chemical and Dynamical Processes in Solution, Spectroscopy in Solution

Molecular Origins of the Apparent Ideal CO Solubilities in Binary Ionic Liquid Mixtures

Utkarsh Kapoor, and Jindal K Shah

J. Phys. Chem. B, Just Accepted Manuscript • Publication Date (Web): 03 Oct 2018

Downloaded from http://pubs.acs.org on October 3, 2018

Just Accepted

"Just Accepted" manuscripts have been peer-reviewed and accepted for publication. They are posted online prior to technical editing, formatting for publication and author proofing. The American Chemical Society provides "Just Accepted" as a service to the research community to expedite the dissemination of scientific material as soon as possible after acceptance. "Just Accepted" manuscripts appear in full in PDF format accompanied by an HTML abstract. "Just Accepted" manuscripts have been fully peer reviewed, but should not be considered the official version of record. They are citable by the Digital Object Identifier (DOI®). "Just Accepted" is an optional service offered to authors. Therefore, the "Just Accepted" Web site may not include all articles that will be published in the journal. After a manuscript is technically edited and formatted, it will be removed from the "Just Accepted" Web site and published as an ASAP article. Note that technical editing may introduce minor changes to the manuscript text and/or graphics which could affect content, and all legal disclaimers and ethical guidelines that apply to the journal pertain. ACS cannot be held responsible for errors or consequences arising from the use of information contained in these "Just Accepted" manuscripts.



Molecular Origins of the Apparent Ideal CO₂ Solubilities in Binary Ionic Liquid Mixtures

Utkarsh Kapoor and Jindal K. Shah*

School of Chemical Engineering, Oklahoma State University, Stillwater, OK 74078 USA

E-mail: jindal.shah@okstate.edu

Abstract

Molecular dynamics simulations were conducted to investigate the variation of Henry's constant of CO₂ in two binary ionic liquid mixtures. One of the mixtures is formed by pairing the cation 1-n-butyl-3-methylimidazolium $[C_4mim]^+$ with chloride Cl^- and methylsulfate $[\mathrm{MeSO_4}]^-$ while the other binary ionic liquid mixture contains [C₄mim]⁺ in combination with the anions Cl⁻ and bis(trifluoromethanesulfonyl)imide [NTf₂]⁻. In order to provide a microscopic understanding of the behavior of the Henry's constant with the anion composition, molecular dynamics simulations of ionic liquid mixtures with and without CO₂ saturation were performed at 353 K and 10 bar. Our calculations indicate that the Henry's constant for CO₂ follows a highly non-linear, although expected based on ideal solubility, trend with respect to the increasing concentration of Cl⁻ in the [C₄mim] Cl_x [NTf₂]_{1-x} while the Henry's constant is almost independent of the anion composition in the $[C_4 mim] Cl_x [MeSO_4]_{1-x}$ system. Structural analyses presented in terms of radial, angular and spatial distribution functions point to significant structural reorganization of the anions around cations in the $[C_4mim]$ Cl_x $[NTf_2]_{1-x}$ system, due to the weakly coordinating ability of the $[NTf_2]^-$ anion with the cation. The [NTf₂]⁻ anion is displaced from the equatorial plane of the imidazolium ring and occupies positions above and below the ring enabling enhanced CO₂-[NTf₂]⁻ association. The rearrangement also weakens the cation π - π interactions resulting in the formation of increased local free volume aiding CO₂ accommodation. On the contrary, such structural transitions are absent in the $[C_4 mim]$ Cl_x $[MeSO_4]_{1-x}$ mixture system.

Introduction

Increasing carbon dioxide (CO₂) emissions has been identified as one of the major environmental concerns. A great deal of effort has been employed for the development of technologies to capture CO₂. At industrial level, the current available processes for the absorption of CO_2 are based on aqueous solutions of alkanolamines and carbonate-based solvents. However, energy intensive operation, high operation costs, corrosion issue and solvent loss due to evaporation or degradation pose a series of disadvantages. ¹ In search of better absorbing solvents, ionic liquids - solvents comprised of molecular ions that frustrate packing and thus existing as liquid under ambient conditions - have emerged as alternative candidates for CO₂ capture and separation. Ionic liquids offer unique advantages in terms of non-volatility, large liquidus range, reasonably good thermal and chemical stability, and high solvation capacity for a wide variety of substances due to their amphiphilic nature. 2-4 Ionic liquids are also regarded as designer solvents as precise modification of their physical, chemical, structural and biological properties can be achieved by a selective combination of cation, anion or their functional groups⁵ and by mixing two ionic liquids.^{6,7} It is also well known that ionic liquids can possess nano-segregated structures comprising of polar and non-polar, the morphology of which can be effectively used as a medium for selective separation of substances.^{8–11}

A large amount of physical solubility data of CO₂ in pure ionic liquids has been reported in the past decade, using both experimental and computational methods, since its first measurement by Blanchard et al.¹² in 1-n-butyl-3-methylimidazolium [C₄mim] hexafluorophosphate [PF₆] at 298.2 K and pressures up to 40 MPa. In a landmark publication by Anthony et al., high CO₂ solubility over O₂ and N₂ was demonstrated, ¹³ which was rationalized on the basis of the interaction of CO₂ with the anion.⁴ It has been established that, for a given cation, the CO₂ solubility is anion-dependent with the cation playing a secondary role unless long alkyl chains are present in the cation. Fluorination of the cation or anion, ^{2,14,15} along with the introduction of ether and carbonyl groups in the cation have also yielded in-

creased physical solubility of CO₂. ¹⁵ Regarding anions the following trend has been observed for the solubility of CO_2 in ionic liquids for a given cation: nitrate $[NO_3]^-$ < thiocyanate $[SCN]^- < methylsulfate [MeSO_4]^- < tetraborofluorate [BF_4]^- < trifluorosulfonate [OTF]^-$ <trifluoroacetate [TFA]^- < [PF $_6$]^- < bis(trifluoromethanesulfonyl)imide [NTf $_2$]^- < perfluoroheptaneacetate $[C_7F_{15}COO]^- < tris(pentafluoroethyl)trifluorophosphate [eFAP]^- <$ $tris(pentafluorobutyl) trifluorophosphate~[bFAP]^-.^{16-18}~An~alternative~theory~for~high~solutions and the solution of the$ bility of CO₂ in ionic liquid was proposed based on the results obtained from molecular dynamics and quantum mechanical calculations. $^{19-22}$ These studies aimed to explain the gas solubility in terms of the existence of free volume in the ionic liquids - the void space between ions. Typically, fluorinated ionic liquids are characterized by weaker cation—anion interactions and possess high molar volumes and free volume, both favorable for CO₂ solubility. Recently, Garrett-Roe, Corcelli, and co-workers studied the CO₂ solvation in the [C₄mim][PF₆] ionic liquid with 2D-infrared spectroscopy and molecular dynamics simulations. The work uncovered enthalpic-driven mechanism of the cavity formation and explained that the CO₂ dissolution occurs because the charges on CO_2 induce reorganization of ions into a favorable solvation shell.²³

Some of the challenges of utilizing fluorinated ionic liquids on an industrial scale include high viscosity and cost relative to nonfluorinated ionic liquids. Blending such ionic liquids with more economical ones may provide an avenue to overcome the disadvantages. The question in such a scenario is the extent to which desirable properties of fluorinated ionic liquids are carried over in binary ionic liquid mixtures and how these properties vary with mixture compositions. Previous studies on binary ionic liquid mixtures have primarily explored thermophysical properties and their classification as ideal or non-ideal mixtures based on the deviation of quantities such as the excess molar volume from the ideal mixing behavior. Detailed exposition of properties of binary ionic liquid mixtures has been dealt with in reviews by Rogers and co-workers, ⁶ and Welton and co-workers. ²⁴

In comparison to a single ionic liquid, investigations focusing on the phase-equilibria properties of CO₂ solubility in binary ionic liquid mixtures are few. The first study measuring the solubility of CO₂ in binary mixture was published by Baltus et al. ²⁵ The authors studied binary ionic liquids formed by mixing the cations 1-octyl-3-methylimidazolium [C₈mim]⁺ with its fluorinated analogue 1-(3,3,4,4,5,5,6,6,7,7,8,8,8-tridecafluorooctyl)-3-methylimidazolium [C₈F₁₃mim]⁺ in the molar ratio 58:42 with [NTf₂]⁻ as the anion. The Henry's constant for CO₂ at 25°C was determined to be 15 bar much closer to the Henry's constant of 4.5 bar for [C₈mim][NTf₂] despite considerable dilution of the ionic liquid with [C₈mim][NTf₂]. The authors remarked that the Henry's constant for the mixture could be calculated using a weighted average but offered no explanation on the molecular level processes leading to the observed behavior.

More recently, Pinto et al. $^{26-28}$ investigated CO₂ solubilities in binary ionic liquid mixtures of 1-ethyl-3-methylimidazolium [C₂mim] ethylsulfate [EtSO₄] - [C₂mim][NTf₂], [C₄mim][EtSO₄] - [C₂mim][NTf₂], ethylpyridinium [C₂py] [EtSO₄] - [C₂mim][NTf₂] at 298.2 K and 1.6 MPa and demonstrated that the CO₂ solubilities in the ionic liquid mixtures were higher than those obtained from the linear mixing rule. The authors speculated that the positive excess molar volumes exhibited by these mixtures correspond to an increase in the free volume explaining CO₂ absorption capacity of the mixtures. Based on COSMO-RS calculations, thermodynamic analysis to predict the Henry's constants of CO₂ in a large number of ionic liquids and subsequent experimental measurements, Moya et al. 29 proposed that the absorption of CO₂ in equimolar mixtures of ionic liquids was more favorable than the linear mixing rule for ionic liquids with unfavorable intermolecular interactions. On the other hand, such enhancements were negligible for ionic liquid mixtures showing near ideal mixing behavior. In a recent study, Hiraga et al. 30 also demonstrated that CO₂ solubilities in the [C₄mim]Cl-[C₄mim][NTf₂] system are higher than ideal mixing predictions.

Although CO₂ solubility measurements in binary ionic liquid mixtures are becoming available, the molecular factors contributing to the (apparent) non-ideal solubility or lack thereof of CO₂ in such mixtures is not well understood, especially for binary ionic liquid mixtures combining a fluorinated and nonfluorinated cation/anion. In a previous study, we analyzed the binary ionic liquid mixtures systems composed of $[C_4mim]Cl-[C_4mim][NTf_2]$ and $[C_4 mim]Cl-[C_4 mim][MeSO_4]$ in terms of thermodynamic, transport and structural properties. Our molecular simulation results indicated that the $[C_4mim]Cl-[C_4mim][NTf_2]$ is an example of binary ionic liquid systems exhibiting positive excess molar volumes over the entire composition region. On the other hand, $[C_4mim]Cl-[C_4mim][MeSO_4]$ exemplifies nearly ideal mixing with small negative excess molar volumes. Although the magnitude of the excess molar volume is small, these systems differ markedly at the molecular level. The distribution of anions around the cation in the $[C_4mim]Cl-[C_4mim][NTf_2]$ system is different from that found in the neat ionic liquids, i. e., the so-called non-native structures emerge. 31 This was not the case for $[C_4 \text{mim}]Cl-[C_4 \text{mim}][MeSO_4]$. As the $[C_4 \text{mim}]Cl-[C_4 \text{mim}][NTf_2]$ system has been shown to display a non-ideal behavior in terms of CO₂ solubility, we hypothesize that the existence of non-native ionic liquid structures may be responsible for the solubility trend.

In order to test our hypothesis, we determine the CO₂ solubility in terms of the Henry's constant as a function of the ionic liquid composition and compare the predictions with a linear mixing rule at 353 K. The deviation from the linearity is then correlated with structural features of the two binary ionic liquid systems mentioned above in the presence of CO₂ at a concentration in the Henry's constant regime using molecular dynamics simulations. We also derive an expression for theoretical Henry's constants for CO₂ in binary ionic liquid mixtures based on the assumption that the absorption of CO₂ is ideal to demonstrate that many experimental observations of non-ideal CO₂ Henry's constants can be directly computed from the knowledge of the Henry's constant for pure ionic liquids. We label this

phenomena as "apparently" ideal, as such behavior can have an entirely different molecular origin than that in the neat ionic liquids as evidenced in this work.

The article is organized as follows. The next section provides details of the force field employed for the ion moieties constituting ionic liquids as well as CO₂. Simulation methodology for calculating Henry's constants using the thermodynamic integration approach followed by protocols to generate well-equilibrated structures with and without CO₂ saturation are described in the Simulation Details section. As the focus of the present article is on investigating the connection between the observed deviation of phase equilibria property behavior and the molecular arrangement of the moieties, the Results and Discussion section is concentrated on the elucidation of the structures in terms of radial, angular and spatial distribution functions along with the coordination number analysis as a function of molar composition. A discussion is included on the origin of apparent excess CO₂ solubilities in terms of Henry's constants observed in binary ionic liquid mixtures. The final section summarizes the conclusions from this work.

Force Field

A classical force field having the following functional form, described by eq. 1, was used for the simulations:

$$E_{\text{tot}} = \sum_{\text{bonds}} K_r (r - r_0)^2 + \sum_{\text{angles}} K_{\theta} (\theta - \theta_0)^2$$

$$+ \sum_{\text{dihedrals}} K_{\chi} [1 + \cos(n\chi - \delta_{\chi})] + \sum_{\text{improper}} K_{\psi} [1 + \cos(n\psi - \delta_{\psi})] +$$

$$+ \sum_{i=1}^{N-1} \sum_{i < j}^{N} \left\{ 4\epsilon_{ij} \left[\left(\frac{\sigma_{ij}}{r_{ij}} \right)^{12} - \left(\frac{\sigma_{ij}}{r_{ij}} \right)^{6} \right] + \left(\frac{q_i q_j}{r_{ij}} \right) \right\}$$

$$(1)$$

where the total energy is expressed in terms of bond stretching, angle bending, dihedral angle torsion, improper, and van der Waals and electrostatic potential. The terms K_r , K_{θ} , K_{χ} , K_{ψ} represent the force constants for the respective bonded interactions while σ_{ij} and ϵ_{ij} the energy and size parameters between atoms i and j in the Lennard-Jones (LJ) 12-6 potential, and q_i is charge on atom i.

For ionic liquids, containing the cation $[C_4 \text{mim}]^+$ and the anions chloride Cl^- , $[\text{MeSO}_4]^-$, and $[\text{NTf}_2]^-$, the force field parameters were obtained from a united atom (UA) force field model developed by Zhong and coworkers. 32,33 The atom type listing is included in Figure S1 of the supporting information. As proposed in this force field model, unlike LJ interactions were computed using the Lorentz-Berthelot combining rule. The intramolecular 1-4 nonbonded interactions, both LJ and electrostatics, were scaled by a factor of 0.5 while the nonbonded interactions between atoms connected by bonds and angles were excluded. Furthermore, non-integer total charge of ± 0.8 is present on the ion moieties. The choice of the force field model was influenced by the fact that we utilized this model in a previous study to interrogate the structure and dynamics of the same binary ionic liquid mixtures studied in this work at ambient pressure conditions. 31 We employed the CO_2 force field model reported in the works of Shi and Maginn, 34 who based their parameterization on the original TraPPE

force field for CO_2 and included flexibility in the bonds and angle.

Simulation Details

Henry's constant

The Henry's constant, k_H , of a solute in solvent, in this study carbon dioxide CO_2 in the ionic liquids and their binary mixtures, was computed using the following relationship:

$$k_H = \rho RT \exp\left(\frac{\mu^{ex}}{k_{\rm B}T}\right) \tag{2}$$

where ρ is the molar density of the pure solvent, R denotes the gas constant, $k_{\rm B}$ and T represent the Boltzmann constant and temperature, respectively; μ^{ex} is the excess chemical potential of the solute referenced to the ideal gas chemical potential at the solvent density. We employed thermodynamic integration to compute the ${\rm CO}_2$ excess chemical potential. In this method, a series of simulations are conducted by varying the interaction strength, from non-interacting to full interaction, between the solute and the solvent through a coupling parameter λ . The free energy change is obtained using eq. 3:

$$\Delta G = \int_0^1 \left\langle \frac{\partial H(\lambda)}{\partial \lambda} \right\rangle d\lambda \tag{3}$$

In this equation, $H(\lambda)$ refers to the Hamiltonian defining state of the system at a given λ . As the CO₂ force field is comprised of both the van der Waals and electrostatic terms, a two-stage thermodynamic integration scheme was adopted. In the first stage, the van der Waals interactions were scaled from the ideal gas state ($\lambda = 0$) to a fully coupled van der Waals state using an equidistant spacing of $\lambda = 0.05$. In the second stage, electrostatic interactions were gradually turned on in an identical manner except that the initial state of CO₂ was that of an interacting solute with van der Waals interactions fully established. A molecular dynamics simulation at each of the λ points was carried out to compute the integrand in eq. 3. The protocol for the equilibration and production runs for these simulations is provided below.

To calculate the Henry's constant, the excess chemical potential of CO₂ solvation was computed in the pure ionic liquids [C₄mim]Cl, [C₄mim][NTf₂], [C₄mim][MeSO₄], and the binary ionic liquid mixtures $[C_4 mim]$ Cl_x $[NTf_2]_{1-x}$, $[C_4 mim]$ Cl_x $[MeSO_4]_{1-x}$ were computed at 353 K and 1 bar using GROMACS 5.0.4. 35,36 Seven mole ratios of the corresponding anions (0:100, 10:90, 25:75, 50:50, 75:25, 90:10 and 100:0) were probed in order to obtain the variation of the Henry's constant as a function of the anion concentration. The initial configurations for each λ value were generated using PACKMOL³⁷ by inserting 1 molecule of CO_2 with 256 (or 250 for 10:90 and 90:10 compositions) ionic liquid pairs in a cubic box with periodic boundary conditions. The initial box sizes were estimated based on our previous work. 31 These configurations were subjected to a steepest descent minimization followed by a 2 ns annealing scheme in which the temperature was changed from 353 to 553 K. Using Langevin dynamics integrator, each system was then equilibrated in canonical (NVT) and isothermal-isobaric (NPT) ensembles for 5 ns each, followed by a production run of 20 ns in the NPT ensemble. A 0.002 ps time step was used for integrating the equations of motion. The temperature and pressure were controlled using a Nosé-Hoover thermostat ($\tau_T = 0.4 \text{ ps}$) and Parrinello-Rahman barostat ($\tau_P = 2.0 \text{ ps}$), respectively. The nonbonded LJ interactions were truncated at 12 Å by applying long range tail corrections while electrostatic interactions were handled using Particle Mesh Ewald (PME) method. The free energy difference or μ^{ex} was evaluated using Bennett Acceptance Ratio (BAR) method³⁸ incorporated as a module in GROMACS. Three independent simulation trials were conducted to determine the statistical uncertainties at each λ .

Molecular Dynamics (MD) Simulations

In order to gain insight into the structural arrangement of CO_2 in the binary ionic liquid systems, additional molecular dynamics simulations of ionic liquid- CO_2 mixtures were carried out. To set the number of CO_2 molecules, the mole fraction in a given binary ionic liquid

system was evaluated at a pressure of 10 bar using eq. 4,

$$x \sim \left(\frac{P}{k_{H,CO_2}}\right) \tag{4}$$

The numerical value of the pressure was selected to permit a relatively large number of CO_2 molecules in the system to reduce statistical uncertainty, yet low enough to ensure the validity of the Henry's Law regime. MD simulations were carried out for ionic liquid systems, both, with and without CO_2 molecules at 10 bar pressure. The low density initial configurations were constructed using a system size of 256 (or 250 for 10:90 and 90:10 anion molar ratios) ion pairs and the corresponding number of CO_2 molecules into a periodic cubic box. The energy of the system was minimized as described above. Again, using the Langevin dynamics integrator, each system was equilibrated in NVT ensemble for a duration of 10 ns. Subsequent equilibration run of 10 ns and production run of 40 ns were carried out in NPT ensemble. All the MD simulations were performed using a time step of 0.002 ps. The handling of the non-bonded interactions was identical to that described above. All the results described below were analyzed using trajectories obtained from the last 20 ns NPT production run saving coordinates every 0.4 ps.

Results and Discussion

Henry's Constants

The Henry's constants of CO_2 , k_{H,CO_2} , in pure ionic liquids $[C_4 mim]Cl$, $[C_4 mim][MeSO_4]$, and $[C_4 mim][NTf_2]$ are predicted to be 179.2 ± 0.0 bar, 181.0 ± 8.1 bar, and 73.4 ± 2.3 bar, respectively. The values indicate that the solubility of CO_2 in these ionic liquids follows the order $[NTf_2]^- > [MeSO_4]^- \sim Cl^-$, for a given cation, which is consistent with the Kamlet-Taft parameter, β , values. 39,40 As shown in Table 1, the Henry's constants for CO_2 in pure ionic liquids were found to be in very good agreement with the experimental values, especially for the $[C_4 mim][NTf_2]$ and $[C_4 mim][MeSO_4]$ ionic liquids. The calculated k_{H,CO_2} for $[C_4 mim]Cl$ is approximately 25% lower than the experimentally reported values, which is probably attributable to the difficulty in measuring CO_2 solubility in the ionic liquid due to its high viscosity.

Figures 1 (a) and (b) show variation of the k_{H,CO_2} with the anion composition for the binary ionic liquid mixture systems, $[C_4 \text{mim}] \text{ Cl}_x \text{ [MeSO_4]}_{1-x}$ and $[C_4 \text{mim}] \text{ Cl}_x \text{ [NTf_2]}_{1-x}$, respectively, at 353 K. The statistical uncertainties are reported from the values obtained by conducting three independent trials as outlined above. The corresponding numerical data are listed in Table S1 of the supporting information. For $[C_4 \text{mim}] \text{ Cl}_x \text{ [NTf_2]}_{1-x}$ system the k_{H,CO_2} values increase with the increase in Cl⁻ mole fraction, suggesting that the solubility of CO_2 decreases as the mixture becomes richer in Cl⁻. The trend is in line with the fact that the Henry's constant of CO_2 is higher for the $[C_4 \text{mim}] \text{Cl}$ ionic liquid than that for $[C_4 \text{mim}] \text{[NTf_2]}$. The Henry's constants in the binary ionic liquid system follow a non-linear curvature. It appears that the system exhibits a negative deviation from the mole fraction weighted linear mixing rule applied to the Henry's constants of the pure ionic liquid with the maximum deviation $(\Delta k_{H,CO_2} \sim -24.4)$ at the equimolar composition, which may imply higher CO_2 solubilities in these binary ionic liquid mixtures than that predicted solely on

the basis of the linear mixing rule. However, as shown in the Supplementary Information, Henry's constants for mixtures can be estimated exclusively on the basis of pure ionic liquids by considering mole fraction weighted harmonic mean of their Henry's constants instead of linear mixing rule. Chen and co-workers¹⁷ also suggested similar lever rule for predicting the mole fraction (solubility) of CO_2 in mixtures based on individual ionic liquids constituting the mixture, which can also be transformed to show that Henry's constants can be calculated by taking weighted harmonic mean of the pure ionic liquid components. Figure 1 (b) clearly display the overlap between the values predicted from the simulations and those determined using the harmonic mixing rule. To further strengthen this view point, we also calculated Henry's constants for the binary mixtures of [C₂mim][NTf₂] - [C₂mim][EtSO₄], $[C_2 mim][NTf_2]$ - $[C_4 mim][EtSO_4]$, and $[C_2 mim][NTf_2]$ - $[C_2 py][EtSO_4]$ using mole fraction weighted harmonic mean of Henry's constants of pure ionic liquids, the results of which are included as Figure S2 of the supporting information along with the actual experimental measurements of Henry's constants reported by Pinto et al. 26,27 It is clearly evident these Henry's constants can be approximated using harmonic mixing rule. Thus, we believe that the Henry's constants for the mixture will always exhibit an apparent non-ideal behavior when compared to a linear mixing rule in cases where the Henry's constants for the pure ionic liquids are significantly different. Further, the experimental measurements 30 of Henry's constants for the identical system of $[C_4mim]$ Cl_x $[NTf_2]_{1-x}$ with three intermediate mole ratios (Cl:[NTf₂] :: 25:75, 50:50, and 75:25) for a temperature range of 333.15 K to 413.15 K are shown graphically in Figure S3 of supporting information, while those at 353 K are included in Figure 1(b). It is evident that the experimental measurements of the Henry's constant also demonstrate a non-linear dependence on the anion concentration and are lower than those obtained assuming a linear mixing rule. It is worth mentioning that predictions for these measurements using mole fraction weighted harmonic rule are not shown, since these values were already predicted using a modified equation of state. Based on the negative deviation from the linear mixing rule, Hiraga et al. 30 suggested that the solubility in the binary ionic liquid system is enhanced and offered the explanation that the enhancement in the solubility of CO_2 for the mixture is caused by a combination of energetic and volume (entropic) effects due to mixing. Below, we rationalize, what we term apparent ideal solubility of CO_2 , in terms of molecular-level structural organization of both the anions which results in structural features that are absent in the pure ionic liquids enabling enhanced the interaction between CO_2 molecules and fluorinated anions ([NTf₂]⁻), (see SDFs and coordination numbers).

Contrary to the $[C_4mim]$ Cl_x $[NTf_2]_{1-x}$ system, the $[C_4mim]$ Cl_x $[MeSO_4]_{1-x}$ system displays ideal mixing behavior for CO_2 solubilities in terms of Henry's constants; k_{H,CO_2} can be predicted using a linear mixing rule. In fact, the values calculated using the harmonic mean approach are identical to the values predicted using linear mixing rule, since the Henry's constants for pure $[C_4mim]Cl$ and $[C_4mim][MeSO_4]$ ionic liquids are very similar. Near ideal CO_2 solubilities in terms of Henry's constants have also been observed previously for binary mixtures of $[C_2mim][NTf_2]$ - $[C_2py][NTf_2]$, 1-butyl-4-methylpyridinium $[C_4mpy][NTf_2]$ - $[C_2py][NTf_2]$, mixtures of $[C_2mim][EtSO_4]$ with $[C_4mim][PF_6]$ and $[C_4mim]$ trifluoroacetate[TFA]. ²⁹ Moya et al. ²⁹ also suggested that weighted average CO_2 gas solubilities, in terms of Henry's constants, can be anticipated for ionic liquid mixtures that possess similarity in cation-anion intermolecular interactions. As reported in a previous study by us, similar cation-anion interactions, expressed in terms of the hydrogen-bonding ability of the anions, lead to microstructures that preserve the cation-anion interactions from the pure ionic liquid systems, ³¹ hinting at the possibility that the presence of native structures in binary ionic liquid mixtures is responsible for the ideal CO_2 solubilities.

Local structure properties: Distribution of CO₂ Molecules in Ionic Liquid Mixtures

To elucidate the underlying connection between the apparent ideal solubility of CO_2 and the structural organization of molecules, trajectories generated from the ionic liquid- CO_2 mixture simulations were analyzed in terms of radial distribution functions (RDFs), spatial distribution functions (SDFs), and angular distribution functions (ADFs) for various molecule - molecule combinations, as explained below. For the following discussion, $[C_4 \text{mim}]^+$ will be referred to as the cation.

Radial Distribution Functions

To investigate the association of CO₂ with different moieties, the center-of-mass (COM)based RDFs between CO₂-anions, CO₂-cation and CO₂-CO₂ are reported. Figure 2 illustrates the organization of CO₂ around the anions as a function of anion concentrations for both the ionic liquid systems. These RDFs indicate a strong localization of CO₂ around the anions, as indicated by the first peak height exceeding the value of 1. The structuring of $\rm CO_2$ around anions is consistent with the hydrogen bond acceptor ability of $\rm Cl^- > [MeSO_4]^ > [NTf_2]^-$ anions, 39,40 advocated by the intensity of the first peak. The locations of the first peak in these RDFs follow the identical order and is indicative of the increasing anion size. The difference in the molecular size and shape of the anions is further reflected in the shape of the first coordination shell. For example, the RDF between CO₂ and spherically symmetric Cl⁻ results in a narrower distribution of CO₂ distances in the first coordination shell. On the other hand, the bulky [MeSO₄]⁻ and [NTf₂]⁻ anions and the presence of multiple CO_2 coordinating sites lead to a more expanded first solvation shell of CO_2 around them. A distinguishing feature of the RDF between the COMs of [NTf₂]⁻ and CO₂ from the other RDFs is the appearance of a split peak in Figure 2 (e) signifying the fact that interaction of CO₂ with [NTf₂]⁻ occurs via multiple binding sites unlike in Cl⁻ or [MeSO₄]⁻. A comparison of RDFs shown in Figures 2(e) and (f), and Figure 3 (b) clearly establishes that [NTf₂]⁻

associates with CO₂ via trifluoromethane (-CF3) group and oxygen atoms. In fact, the asymmetric nature of CO₂ binding with fluorinated anions has been previously suggested in terms of molecular electrostatic potential which is guided by the interplay of, both, electrostatic interaction between carbon of CO₂ and fluorines as well as halogen-bonding between oxygen of CO₂ and fluorines. ⁴¹ We will revert to this bidentate modality of the anion while discussing the coordination number.

The cation-CO₂ RDFs presented in Figure S4 panels (a) and (b) reinforce that the cation has a lower affinity for CO₂ in comparison to the anion. This fact is borne out by a peak intensity slightly greater than 1 in the first solvation shell and nearly homogenous distribution of CO₂ in the second coordination sphere and thereafter. For both the ionic liquid mixture systems, the location of the first peak distance in the RDFs remains nearly constant. Further, the peak position shows a weak dependence on the molar composition of anions, suggesting that cation-CO₂ interactions are largely unperturbed irrespective of the anion identity. However, compaction of first solvation shell with increasing Cl⁻ concentration and presence of a second peak, the trends of which can be compared with cation-anion RDFs (Figures. S5 and S6), reveals that CO₂ association with the cation is dictated by the strong CO₂-anion interaction.

Coordination Numbers

As clearly evident in Figures 2 (a) - (f), the first peak intensity in all the CO₂-anion RDFs bears a weak dependence on the anion concentration, pointing to the CO₂-anion association that is independent of the dilution of one anion with respect to the other. Given that the RDF value at a given distance from the central molecule is obtained as the ratio of the local number density to that of the bulk density and the CO₂ bulk density changes considerably over different ionic liquid mixtures, the coordination of CO₂ molecules must be altered to a significant extent in order to maintain a similar association. Figure 4 presents the coordination numbers, in the respective first solvation shells, of CO₂ with respect to the COM

and specific sites of the anions in both the binary ionic liquid mixture systems as a function of molar composition. The number of CO_2 molecules around a Cl^- anion ranges between 1-2 over the entire composition range for both the mixture systems with a key difference: the number of CO_2 molecules coordinated to Cl^- in the $[C_4mim]$ Cl_x $[MeSO_4]_{1-x}$ system is approximately constant with a value close to 1.5. On the other hand, the number of CO_2 molecules found in the first coordination shell around a Cl^- anion increases steadily from 1 at the lowest Cl^- concentration to approximately 2 in the $[C_4mim]$ Cl_x $[NTf_2]_{1-x}$ system. Similarly, for the $[MeSO_4]^-$ anion, the overall coordination number of CO_2 is ~ 2 with very weak dependence on the anion concentration. Near constancy of the CO_2 coordination numbers is attributed to the fact that the distribution of anions around the cation in the $[C_4mim]$ Cl_x $[MeSO_4]_{1-x}$ mixture system deviates very little as a function of the molar composition of the anion (Figure S5 of the supporting information). As expected, the trend for the number of CO_2 molecules around the oxygen atoms in these systems mirrors that obtained for the CO_2 molecules around the primary association sites for CO_2 .

A very different picture emerges for the CO_2 distribution in the $[C_4 mim]$ Cl_x $[NTf_2]_{1-x}$ system. The most striking feature is that the coordination number of CO_2 with $[NTf_2]^-$, which increases from 4 to \sim 7 with the increase in the Cl^- concentration. The origin of such a dramatic change in the coordination number can be traced to the number of CO_2 molecules located around the anion moieties - CF_3 and oxygen. As can be noted from Figure 4 (b), the number of CO_2 molecules around the trifluoromethane (- CF_3) group increases from 3 to 5 as Cl^- is added to the system. Unlike this behavior, only one CO_2 molecule is observed to interact with oxygen atom at any composition, clearly suggesting that the increase in average number of CO_2 molecules around $[NTf_2]^-$ can be rationalized in terms of an enhanced interaction with (- CF_3) group or fluorine atoms. In fact, the enhancement in CO_2 - CF_3 interaction is further advocated by the decreasing interaction between the cation and the - CF_3 group, evident as decreasing first peak height and near isotropic distribution

for all the solvation shells, with the increasing Cl⁻ concentration, as shown in Figure 3 (a). Thus, it believed that this reduction in cation-CF3 interaction allows fluorine atoms to become increasingly accessible to interact with with CO₂.

Further, in line with the COM based cation-CO₂ RDFs, the coordination numbers listed in Table S2 of the supporting information reveal that the first solvation shell of the cation is occupied by \sim 4-5 CO₂ molecules, which is nearly same as that of the anions as shown in Figure S7 of the supporting information. This, again, corroborates that the association of CO₂ with the anion dictates the cation-CO₂ interaction. Additionally, interaction of CO₂ with both anion and cation also influences the association of different CO₂ molecules to a significant extent. The inspection of CO₂-CO₂ COM-based RDFs (Figure S8 of the supporting information) shows local enhancement of CO₂ \sim 2.5 times the bulk density with coordination number of \sim 3 (Table S2 of the supporting information) in both the ionic liquid mixture systems, as opposed to the bulk CO₂ phase where 9.1 nearest CO₂ neighbors are anticipated.²²

Spatial Distribution Functions

More details about the relative positions of CO_2 molecules around an anion can be collected from the three-dimensional spatial distribution functions (SDFs) depicted in Figure 5 and Figure 6. These SDFs were generated at the isosurface densities twice the corresponding bulk density. In the $[C_4\text{mim}]$ Cl_x $[MeSO_4]_{1-x}$ mixture system, CO_2 occupies two distinct high density regions around $[MeSO_4]^-$: (a) along the sulfur-oxygen vector; (b) along the bisector of the oxygen-sulfur-oxygen bond angle. The locations of these enhanced density areas correspond to the first and second peaks obtained in the $[MeSO_4]$ - CO_2 RDFs (Figure 2 (c)), respectively. It can be deduced from the Figure S9 of the supporting information that a large fraction of the CO_2 molecules in the two regions are situated in the plane of three equivalent oxygen atoms of $[MeSO_4]^-$. The structural diversity or transition in these SDFs is almost

non-existent at all the concentrations except at the mole ratio of 75:25 at which the high density regions disappear. However, computing the SDF at a lower isosurface density (1.7 times the bulk density) restores the most likely positions CO_2 is expected to occupy (Figure S10 of the supporting information. For consistency, the SDFs for $[C_4\text{mim}]$ Cl_x $[NTf_2]_{1-x}$ system at 1.7 times the bulk density are depicted in Figure S11 of the supporting information). This behavior can be expected after visualizing the respective RDFs, where both the first and second peaks identified in Figure 2 (b) and (c) reduce considerably for x_{Cl} =0.75. We have been able to reproduce the reduction in peak heights by conducting two additional independent simulations. At this point, it is unclear why such a behavior is observed only at this particular composition. Interestingly, small changes in the SDFs are discernible for the areas occupied along the bisector of the two equivalent oxygen atoms which is probably due to minute fluctuations seen in the RDFs. Taken together, the SDFs help explain the invariance in the coordination number of CO_2 around $[MeSO_4]^-$ along the entire composition range (Figure 4) which in turn provides a rationale for the weak dependence of CO_2 Henry's constants on the anion composition.

Similar to $[C_4 mim]$ Cl_x $[MeSO_4]_{1-x}$ system, for $[C_4 mim]$ Cl_x $[NTf_2]_{1-x}$ mixtures there are two types of high density areas of CO_2 around $[NTf_2]^-$ that arise due to the interaction of CO_2 with both trifluoromethane (-CF3) group and four equivalent oxygen atoms. Nevertheless, unlike $[C_4 mim]$ Cl_x $[MeSO_4]_{1-x}$ system structural transitions are visual in the $[C_4 mim]$ Cl_x $[NTf_2]_{1-x}$ mixture system as the Cl^- concentration is increased (Figure 6). For the pure $[C_4 mim][NTf_2]$ system, the CO_2 coordinates with $[NTf_2]^-$ with three sites and the isosurface density region is situated farther than that for $[MeSO_4]^-$, in line with the observation made in the CO_2 -anion RDFs. For the lowest Cl^- concentration (x_{Cl} =0.10), a slight enhancement in the CO_2 densities (middle region and the area towards the right, when compared with pure $[C_4 mim][NTf_2]$ system) is visible along with an additional site. This signifies that even the smallest addition of Cl^- , which displaces $[NTf_2]^-$ from the ring binding sites, 31,42

is beneficial for the interaction of CO₂ with the weakly coordinating anion [NTf₂]⁻. As the concentration of Cl⁻ is further increased, there is a noticeable intensification around all the four sites. Again, it is worth mentioning that such CO₂-[NTf₂] interactions may not be discernible with the visualization of RDFs. However, weak concentration dependence of CO₂-anion RDFs as compared to cation-anion RDFs provides clues that interaction between CO₂ and anions are significantly increased in order to maintain the local density.

These above mentioned result supports previous investigations speculation that the nature of anion and its dominant interaction with CO_2 has a significant effect in determining solubility in ionic liquids than the cation.

Effect of CO₂ on the structure of ionic liquids

In order to determine the influence of CO_2 absorption on the microstructure of ionic liquid systems, COM-based RDFs elucidating cation-anion interactions and center-of-ring (COR) RDFs for unraveling the cation-cation interactions were computed for ionic liquid mixtures with and without CO_2 saturation. The resulting RDFs are provided in Figures S5 and S6 of the supporting information. Comparing the RDFs with and without CO_2 molecules clearly shows that the molecular structure of the ionic liquid system remains unperturbed upon the addition of CO_2 except for a very minute displacement in the pre-peak, at \sim 4-5 Å, of cation-cation COR RDFs. For the $[C_4 mim] Cl_x [NTf_2]_{1-x}$ mixture system, these changes can be easily visualized using cation-anion and cation-cation coordination numbers reported in Figure S7 of the supporting information. As expected, cation-anion coordination numbers for ionic liquid mixtures with and without CO_2 saturation are almost identical, while a small but noticeable reduction in the coordination number of cation with respect to another cation can be detected in the presence of CO_2 . As an aside, the juxtaposition of the RDFs of the system without CO_2 saturation with those reported in our previous study 31 indicates that the structures of binary ionic liquid mixtures undergoes minimal changes with the increase

in pressure, consistent with the incompressible nature of these systems. ^{21,43}

To further scrutinize the above-mentioned change in the cation-cation coordination numbers, the relative orientational distribution in the form of ADFs, for the cations, anions and the CO_2 molecule around the cation in the respective first solvation shell were computed. The coordinate system for these calculations was fixed at the center of the imidazolium ring and is sketched in Figure S12 of the supporting information. The ADFs were computed for the angles designated as θ and and ϕ ; the polar angle θ is the angle between the ring normal and the vector connecting the COM of an anion or CO₂ molecule and COR, while the azimuthal angle ϕ is defined with respect to the vector joining the COR to the nitrogen bonded to the first carbon atom in the butyl chain.

Figures 7 (a)-(f) provide the probability of occurrence of the polar and azimuthal angles of anions and CO_2 molecules around cations in the binary ionic liquid system of $[C_4 \text{mim}]$ Cl_x $[NTf_2]_{1-x}$ with and without CO_2 . The ADFs for the strongly interacting and small size $Cl^$ are rather insensitive to the presence of CO_2 molecules. However, subtle rearrangements in the relative orientations of the larger anions are noticeable in the 0-30 and 150-180 degree regions. Such changes are more pronounced for the weakly associating [NTf₂]⁻ in comparison to that seen for the $[MeSO_4]^-$ anion (Figure X of the supporting information). CO_2 molecules are preferentially located above or below the imidazolium ring and associate from the cationic tail site ($\phi \sim 0$ -60), which is not easily accessible for the cation-anion interaction. The weak association of CO₂ with cation and occupancy of CO₂ above and below the ringplane is in agreement with previous studies. 22,43 It can be inferred from Figure S14 of the supporting information that, for both the ionic liquid systems, the neighboring cations are involved in π - π stacking. The orientation of cations around cation is not markedly affected by the presence of CO₂ molecules. However, it is worth mentioning that change in the molar composition of Cl⁻ ion leads to subtle angular re-organization of anions around cations, even for the ionic liquid mixture systems without CO₂ molecules.³¹ Thus, the molecular picture in these systems is that the positioning of CO₂ and large size weakly coordinating anion results in a partial shielding of the cation-cation interactions, causing the reduction in cation-cation coordination numbers. Furthermore, similar angular preferences of the CO₂ and [NTf₂]⁻ is responsible for the CO₂-anion interactions and can explain the increasing coordination number of CO₂ around [NTf₂]⁻ as Cl⁻ concentration increases. The decrease in the association between the cation and the [NTf₂]⁻ as inferred from the RDFs and SDFs is also likely to lead an increase in the free volume in which CO₂ molecules can be inserted.

The invariance of the cation-anion RDFs between the neat and CO₂ containing ionic liquid systems has been previously reported. For example, Huang et al. ²² discovered that although the cation-anion RDFs do not change in the presence of CO₂, that the anion tends to shift towards the plane of the imidazolium ring thereby increasing the local free volume in which CO_2 can reside. Klähn and Seduraman²¹ examined a number of ionic liquids with varying cation-anion interaction strengths and found that the weaker is the interaction, the greater is the void space in these ionic liquids. However, the volume of the largest cavities is smaller than the volume of a CO_2 molecule. Therefore, subtle reorganizations of the ions is necessary to create void space large enough for CO₂ positioning. Based on the angular preferences exhibited by the weakly coordinating [NTf₂]⁻, we surmise that empty spaces are generated around [NTf₂]⁻. The appearance of an entirely new high density region in the SDF of CO₂ around $[NTf_2]^-$ is most likely due to this phenomena.

Partial molar volumes, \bar{V}_i , were determined for CO₂ as a function of molar composition in both the ionic liquid mixture systems. The values are listed in Table S3 of the supporting information along with the simulation volumes of ionic liquid systems with and without CO₂ saturation. In general, \bar{V}_i values of CO₂ in ionic liquids and their mixtures at the saturation concentration lie within 44 - 46 cm³/mol, which is at the lower limit of the conventional organic solvents, where \bar{V}_i ranged from 45 to 53 cm³/mol.⁴⁴ However, available literature data of calculated \bar{V}_i values of CO₂ for pure ionic liquids containing [C₄mim]⁺, as the cation, were found in the range of 36 - 37 cm³/mol for a number of anions including Cl⁻ and [NTf₂]⁻,²¹ and [MeSO₄]⁻.⁴⁵ This difference in values can be attributed not only to the fact that \bar{V}_i depends on the temperature, pressure and concentration of the solute but also different force fields and simulation protocols. Nevertheless, $\bar{V}_i > 0$ for all the ionic liquid mixture systems indicates an expansion in ionic liquid volume at the conditions described here, which is also likely to contribute to the formation additional free volume in these systems.

Hence, from the results presented in this study, it is possible to provide a molecular reasoning of the apparent ideal solubility behavior in the binary ionic liquid mixture [C₄mim] Cl_x [NTf₂]_{1-x}. Our previous study demonstrated that a binary mixture of ionic liquids containing a common cation and anions with significant difference in hydrogen bond ability and sizes undergoes structural transitions as the anion composition is varied and molecular structures non-native to the neat ionic liquid analogues are produced. These non-native structures are characterized by the occupancy of the stronger coordinating anion in the place of the imidazolium ring, while the weakly associating anion is displaced to the regions above and below the plane.³¹ The repositioning of the anions also causes small but perceptible changes in the angular arrangement of the weakly coordinating anion, possibly increasing the number of voids or the volume of the voids between the cation and [NTf₂]⁻. ³¹ Further anion reorganization of the anions around the cation occurs in the presence of CO₂ which expands unoccupied volume and leads to CO₂ positions above and below the imidazolium ring plane enhancing the interaction with [NTf₂]⁻. The lack of such structural features in $[C_4 mim] Cl_x [MeSO_4]_{1-x}$ mixture system implies that the CO_2 dissolution mechanism does not differ from that observed for the pure ionic liquid systems leading to ideal behavior.

Conclusion

Two binary ionic liquid mixtures, namely, $[C_4 mim] Cl_x [NTf_2]_{1-x}$ and $[C_4 mim] Cl_x [MeSO_4]_{1-x}$ were investigated at different molar composition ratios of anions (0:100, 10:90, 25:75, 50:50, 75:25, 90:10, 100:0) for their ability to absorb CO₂ with the objective of establishing an interconnection between the observed Henry's constant and the microstructure of ionic liquid mixtures. For this purpose, molecular dynamics simulations were conducted at a temperature of 353 K to compute Henry's constants using the thermodynamic integration approach.

The Henry's constants of CO_2 in $[C_4mim]$ Cl_x $[MeSO_4]_{1-x}$ were observed to follow a linear mixing rule for the entire composition range while negative deviations from the mole fraction weighted linear mixing rule were found for $[C_4 mim] Cl_x [NTf_2]_{1-x}$ mixture system with maximum deviation at equimolar composition. In order to understand the contrasting behavior, simulations were performed at a temperature and pressure of 353 K and 10 bar for all the systems with and without CO₂ saturation to obtain structural difference in these systems when CO_2 in introduced. The molecular structure was elucidated in terms of the radial distribution functions (RDFs), angular distribution functions (ADFs), spatial distribution functions (SDFs), and coordination numbers of CO₂ around the anions.

In $[C_4 mim]$ Cl_x $[NTf_2]_{1-x}$ mixture system, higher solubility of CO_2 than that predicted by a linear mixing rule is primarily due to enhanced CO₂-[NTf₂]⁻ interaction suggested by a weak concentration dependence of CO₂-[NTf₂] center-of-mass (COM) RDF. This is, however, not the case for the cation-anion RDFs. The coordination number of CO₂ with respect to [NTf₂]⁻ increases with an increase in Cl⁻ concentration, the behavior that was traced back to the increased propensity for CO_2 to interact with the trifluoromethane (-CF₃) site in [NTf₂]⁻. It was also demonstrated that the coordination numbers of CO₂ around -CF₃ closely parallel to those computed for the [NTf₂]⁻ anion. This is also advocated by the appearance of a new spatial region for CO_2 -anion association in the SDFs. Unlike $[C_4mim]$ Cl_x $[NTf_2]_{1-x}$ system, $[C_4mim]$ Cl_x $[MeSO_4]_{1-x}$ mixture system lacks noticeable enhancement in CO_2 -anion association explaining the ideal behavior for the Henry's constants.

For both the mixtures, the underlying cation-anion interactions do not seem to be perturbed when the COM cation-anion RDFs are compared with and without CO_2 . However, the spatial arrangement of anions in the $[C_4 \text{mim}]$ Cl_x $[NTf_2]_{1-x}$ system undergoes dramatic changes with increasing Cl^- concentration as reported in our previous study³¹ such that the stronger coordinating ability of Cl^- leads to a displacement of $[NTf_2]^-$ from the plane of the imidazolium ring; the preferred locations for $[NTf_2]^-$ becoming increasingly above and below the plane of the imidazolium ring. We believe that such structural transitions permit $[NTf_2]^-$ to interact more favorably with CO_2 as demonstrated in this work. The absence of reorganization of anions in the $[C_4 \text{mim}]$ Cl_x $[MeSO_4]_{1-x}$ mixture system does not provide opportunities for such non-native interactions with CO_2 . The rearrangement of the anion can also be deduced by comparing ADFs for systems with and without CO_2 solvation. It is likely that small angular displacements of anions in the presence of CO_2 also generate free volume in which CO_2 can be accommodated.

Overall, we speculate that binary ionic liquid mixtures comprising of anions with significant differences in size, molar volumes and hydrogen bonding ability will potentially display negative deviations from a linear mixing rule for the Henry's constants. Efforts are currently underway to exploit this strategy to design binary ionic liquid mixtures exhibiting significant perturbations in their microstructure from the corresponding neat ionic liquids and fine-tune the absorption of CO_2 .

Acknowledgement

This material is based upon work supported by the National Science Foundation (NSF) Award Number CBET-1706978. The authors gratefully acknowledge partial funding from the Oklahoma State University. The computing for this project was performed at the OSU High Performance Computing Center at Oklahoma State University supported in part through the National Science Foundation grant OCI-1126330.

Supporting Information Available

Supporting information includes Henry's constants, simulation volumes, partial molar volumes raw data at 353 K along with the plots of temperature dependence of Henry's constant of CO_2 in $[C_4mim]$ Cl_x $[NTf_2]_{1-x}$ obtained from literature, radial distribution functions (RDFs) and angular distribution functions (ADFs) of anions around the cation, with and without CO_2 saturation, and spatial distribution functions (SDFs) of CO_2 molecules around anions at a lower isosurface density. Also included are the chemical structure schematic, with atom numbering and coordinate system used for ADFs calculation. This material is available free of charge via the Internet at http://pubs.acs.org/.

References

- (1) White, C. M.; Strazisar, B. R.; Granite, E. J.; Hoffman, J. S.; Pennline, H. W. Separation and Capture of CO₂ from Large Stationary Sources and Sequestration in Geological Formations—Coalbeds and Deep Saline Aquifers. J. Air Waste Manage. Assoc. 2003, 53, 645–715.
- (2) Anderson, J. L.; Dixon, J. K.; Brennecke, J. F. Solubility of CO₂, CH₄, C₂H₆, C₂H₄, O₂, and N₂ in 1-Hexyl-3-methylpyridinium Bis(trifluoromethylsulfonyl)imide: Comparison to Other Ionic Liquids. Acc. Chem. Res. 2007, 40, 1208–1216.

- (3) Freemantle, M. An Introduction to Ionic Liquids, 1st ed.; The Royal Society of Chemistry: Cambridge, U.K., 2010.
- (4) Cadena, C.; Anthony, J. L.; Shah, J. K.; Morrow, T. I.; Brennecke, J. F.; Maginn, E. J. Why is CO₂ so Soluble in Imidazolium-Based Ionic Liquids? *J. Am. Chem. Soc.* 2004, 126, 5300–5308.
- (5) Stark, A.; Seddon, K. R. *Ionic Liquids, 5th ed.*; Seidel, A. (Ed.), Kirk-Othmer Encyclopedia of Chemical Technology, vol. 26; Wiley, Hoboken, 2007.
- (6) Chatel, G.; Pereira, J. F. B.; Debbeti, V.; Wang, H.; Rogers, R. D. Mixing ionic liquids

 "simple mixtures" or "double salts"? *Green Chem.* **2014**, *16*, 2051–33.
- (7) Kapoor, U.; Shah, J. K. Thermophysical Properties of Imidazolium-Based Binary Ionic Liquid Mixtures Using Molecular Dynamics Simulations. J. Chem. Eng. Data 2018, 63, 2512–2521.
- (8) Kapoor, U.; Shah, J. K. Globular, Sponge-like to Layer-like Morphological Transition in 1-n-Alkyl-3-methylimidazolium Octylsulfate Ionic Liquid Homologous Series. *J. Phys. Chem. B* **2017**, *122*, 213–228.
- (9) Kapoor, U.; Shah, J. K. Effect of Molecular Solvents of Varying Polarity on the Self-Assembly of 1-n-Dodecyl-3-methylimidazolium Octylsulfate Ionic Liquid. J. Theor. Comput. Chem 2018, 17, 1840004.
- (10) Hayes, R.; Warr, G. G.; Atkin, R. Structure and Nanostructure in Ionic Liquids. *Chem. Rev.* **2015**, *115*, 6357–6426.
- (11) Lozano, P.; Bernal, J. M.; Garcia-Verdugo, E.; Sanchez-Gomez, G.; Vaultier, M.; Burguete, M. I.; Luis, S. V. Sponge-Like Ionic Liquids: A New Platform for Green Biocatalytic Chemical Processes. *Green Chem.* 2015, 17, 3706–3717.

- (12) Blanchard, L. A.; Brennecke, J. F. Green Processing using Ionic Liquids and CO₂.

 Nature 1999, 399, 28–29.
- (13) Anthony, J. L.; Maginn, E. J.; Brennecke, J. F. Solubilities and Thermodynamic Properties of Gases in the Ionic Liquid 1-n-Butyl-3-methylimidazolium Hexafluorophosphate.

 J. Phys. Chem. B 2002, 106, 7315–7320.
- (14) Almantariotis, D.; Stevanovic, S.; Fandiño, O.; Pensado, A. S.; Padua, A. A. H.; Coxam, J. Y.; Costa Gomes, M. F. Absorption of Carbon Dioxide, Nitrous Oxide, Ethane and Nitrogen by 1-Alkyl-3-methylimidazolium (C_nmim, n= 2,4,6) Tris(pentafluoroethyl)trifluorophosphate Ionic Liquids (eFAP). J. Phys. Chem. B **2012**, 116, 7728–7738.
- (15) Muldoon, M. J.; Aki, S. N. V. K.; Anderson, J. L.; Dixon, J. K.; Brennecke, J. F. Improving Carbon Dioxide Solubility in Ionic Liquids. J. Phys. Chem. B 2007, 111, 9001–9009.
- (16) Ramdin, M.; de Loos, T. W.; Vlugt, T. J. H. State-of-the-Art of CO₂ Capture with Ionic Liquids. *Ind. Eng. Chem. Res.* **2012**, *51*, 8149–8177.
- (17) Lei, Z.; Dai, C.; Chen, B. Gas Solubility in Ionic Liquids. *Chem. Rev.* **2014**, *114*, 1289–1326.
- (18) Zeng, S.; Zhang, X.; Bai, L.; Zhang, X.; Wang, H.; Wang, J.; Bao, D.; Li, M.; Liu, X.; Zhang, S. Ionic-Liquid-Based CO₂ Capture Systems: Structure, Interaction and Process. Chem. Rev. 2017, 117, 9625–9673.
- (19) Babarao, R.; Dai, S.; Jiang, D.-e. Understanding the High Solubility of CO₂ in an Ionic Liquid with the Tetracyanoborate Anion. J. Phys. Chem. B **2011**, 115, 9789–9794.
- (20) Zhang, X.; Liu, X.; Yao, X.; Zhang, S. Microscopic Structure, Interaction, and Proper-

- ties of a Guanidinium-Based Ionic Liquid and Its Mixture with CO_2 . Ind. Eng. Chem. Res. **2011**, 5θ , 8323–8332.
- (21) Klähn, M.; Seduraman, A. What Determines CO₂ Solubility in Ionic Liquids? A Molecular Simulation Study. *J. Phys. Chem. B* **2015**, *119*, 10066–10078.
- (22) Huang, X.; Margulis, C. J.; Li, Y.; Berne, B. J. Why is the Partial Molar Volume of CO₂ so Small When Dissolved in a Room Temperature Ionic Liquid? Structure and Dynamics of CO₂ Dissolved in [bmim]⁺ [PF₆]⁻. J. Am. Chem. Soc. **2005**, 127, 17842–17851.
- (23) Daly Jr., C. A.; Brinzer, T.; Allison, C.; Garrett-Roe, S.; Corcelli, S. A. Enthalpic Driving Force for the Selective Absorption of CO 2by an Ionic Liquid. *J. Phys. Chem. Lett.* **2018**, *9*, 1393–1397.
- (24) Niedermeyer, H.; Hallett, J. P.; Villar-Garcia, I. J.; Hunt, P. A.; Welton, T. Mixtures of Ionic Liquids. *Chem. Soc. Rev.* **2012**, *41*, 7780–23.
- (25) Baltus, R. E.; Culbertson, B. H.; Dai, S.; Luo, H.; DePaoli, D. W. Low-Pressure Solubility of Carbon Dioxide in Room-Temperature Ionic Liquids Measured with a Quartz Crystal Microbalance. J. Phys. Chem. B 2004, 108, 721–727.
- (26) Pinto, A. M.; Rodríguez, H.; Colón, Y. J.; Arce Jr., A.; Arce, A.; Soto, A. Absorption of Carbon Dioxide in Two Binary Mixtures of Ionic Liquids. *Ind. Eng. Chem. Res.* **2013**, 52, 5975–5984.
- (27) Pinto, A. M.; Rodríguez, H.; Arce, A.; Soto, A. Carbon Dioxide Absorption in the Ionic Liquid 1-Ethylpyridinium Ethylsulfate and in its Mixtures with Another Ionic Liquid. Int. J. Greenhouse Gas Control 2013, 18, 296–304.
- (28) Pinto, A. M.; Rodríguez, H.; Arce, A.; Soto, A. Combined Physical and Chemical

- Absorption of Carbon Dioxide in A Mixture of Ionic Liquids. *J. Chem. Thermodyn.* **2014**, 77, 197–205.
- (29) Moya, C.; Gonzalez-Miquel, M.; Rodríguez, F.; Soto, A.; Rodríguez, H.; Palomar, J. Non-ideal Behavior of Ionic Liquid Mixtures to Enhance CO₂ Capture. Fluid Phase Equilib. 2017, 450, 175–183.
- (30) Hiraga, Y.; Koyama, K.; Sato, Y.; Smith Jr., R. L. Measurement and Modeling of CO₂ Solubility in [bmim]Cl – [bmim][Tf₂N] Mixed-Ionic Liquids for Design of Versatile Reaction Solvents. J. Supercrit. Fluids 2018, 132, 42–50.
- (31) Kapoor, U.; Shah, J. K. Preferential Ionic Interactions and Microscopic Structural Changes Drive Nonideality in Binary Ionic Liquid Mixtures as Revealed from Molecular Simulations. *Ind. Eng. Chem. Res.* **2016**, *55*, 13132–13146.
- (32) Liu, Z.; Chen, T.; Bell, A.; Smit, B. Improved United-Atom Force Field for 1-Alkyl-3-methylimidazolium Chloride. J. Phys. Chem. B 2010, 114, 4572–4582.
- (33) Zhong, X.; Liu, Z.; Cao, D. Improved Classical United-Atom Force Field for Imidazolium-Based Ionic Liquids: Tetrafluoroborate, Hexafluorophosphate, Methylsulfate, Trifluoromethylsulfonate, Acetate, Trifluoroacetate, and Bis(trifluoromethylsulfonyl)amide. J. Phys. Chem. B 2011, 115, 10027–10040.
- (34) Shi, W.; Maginn, E. J. Atomistic Simulation of the Absorption of Carbon Dioxide and Water in the Ionic Liquid 1-n-Hexyl-3-methylimidazolium Bis(trifluoromethylsulfonyl)imide ([hmim][Tf₂N]). J. Phys. Chem. B **2008**, 112, 2045–2055.
- (35) Abraham, M. J.; van der Spoel, D.; Lindahl, E.; Hess, B. GROMACS User Manual Version 5.0.4, www.gromacs.org.

- (36) Lindahl, E.; Hess, B.; van der Spoel, D. GROMACS 3.0: A Package for Molecular Simulation and Trajectory Analysis. *Molec. Model. Ann.* **2001**, *7*, 306–317.
- (37) Martínez, L.; Andrade, R.; Birgin, E. G.; Martínez, J. M. PACKMOL: A Package for Building Initial Configurations for Molecular Dynamics Simulations. J. Comput. Chem. 2009, 30, 2157–2164.
- (38) Bennett, C. H. Efficient Estimation of Free Energy Differences from Monte Carlo Data.

 J. Comput. Phys. 1976, 22, 245–268.
- (39) Lungwitz, R.; Spange, S. A Hydrogen Bond Accepting (HBA) Scale For Anions, Including Room Temperature Ionic Liquids. *New J. Chem.* **2008**, *32*, 392–394.
- (40) Lungwitz, R.; Strehmel, V.; Spange, S. The Dipolarity/Polarisability of 1-Alkyl-3-Methylimidazolium Ionic Liquids as Function of Anion Structure and the Alkyl Chain Length. New J. Chem. 2010, 34, 1135–1140.
- (41) Rao, S. S.; Gejji, S. P. CO_2 Absorption Using Fluorine Functionalized Ionic Liquids: Interplay of Hydrogen and σ -Hole Interactions. *J. Phys. Chem. A* **2016**, *120*, 1243–1260.
- (42) Matthews, R. P.; Villar-Garcia, I. J.; Weber, C. C.; Griffith, J.; Cameron, F.; Hallett, J. P.; Hunt, P. A.; Welton, T. A Structural Investigation of Ionic Liquid Mixtures. Phys. Chem. Chem. Phys. 2016, 18, 8608–8624.
- (43) Zhang, X.; Huo, F.; Liu, Z.; Wang, W.; Shi, W.; Maginn, E. J. Absorption of CO₂ in the Ionic Liquid 1-n-Hexyl-3-methylimidazolium Tris(pentafluoroethyl)trifluorophosphate ([hmim][FEP]): A Molecular View by Computer Simulations. J. Phys. Chem. B 2009, 113, 7591–7598.
- (44) Klähn, M.; Martin, A.; Cheong, D. W.; Garland, M. V. Variation and Decomposition of

- the Partial Molar Volume of Small Gas Molecules in Different Organic Solvents Derived From Molecular Dynamics Simulations. *J. Chem. Phys.* **2013**, *139*, 244506.
- (45) Kumelan, J.; Pérez-Salado Kamps, Á.; Tuma, D.; Maurer, G. Solubility of Carbon Dioxide in Liquid Mixtures of Water + [bmim][CH₃SO₄]. *J. Chem. Eng. Data* **2011**, 56, 4505–4515.
- (46) Taguchi, R. Measurement and Calculation of High Pressure CO₂ Solubilities in Functional Ionic Liquids. M.S., Thesis, Graduate School of Environmental Studies, Tohoku University, 2009,
- (47) Jang, S.; Cho, D.-W.; Im, T.; Kim, H. High-pressure Phase Behavior of $CO_2 + 1$ -Butyl-3-methylimidazolium Chloride System. Fluid Phase Equilib. **2010**, 299, 216–221.
- (48) Kumelan, J.; Pérez-Salado Kamps, Á.; Tuma, D.; Maurer, G. Solubility of CO₂ in the Ionic Liquids [bmim][CH₃SO₄] and [bmim][PF₆]. *J. Chem. Eng. Data* **2006**, *51*, 1802–1807.
- (49) Raeissi, S.; Peters, C. J. Carbon Dioxide Solubility in the Homologous 1-Alkyl-3-methylimidazolium Bis(trifluoromethylsulfonyl)imide Family. *J. Chem. Eng. Data* **2009**, *54*, 382–386.
- (50) Carvalho, P. J.; Álvarez, V. H.; Marrucho, I. M.; Aznar, M.; Coutinho, J. A. P. High Pressure Phase Behavior of Carbon Dioxide in 1-Butyl-3-methylimidazolium Bis(trifluoromethylsulfonyl)imide and 1-Butyl-3-methylimidazolium Dicyanamide Ionic Liquids. J. Supercrit. Fluids 2009, 50, 105–111.
- (51) Jacquemin, J.; Husson, P.; Majer, V.; Costa Gomes, M. F. Influence of the Cation on the Solubility of CO₂ and H₂ in Ionic Liquids Based on the Bis(trifluoromethylsulfonyl)imide Anion. *J. Solution Chem.* **2007**, *36*, 967–979.

Table 1: Comparison of Henry's constants k_{H,CO_2} for CO_2 of pure ionic liquids, obtained from simulations in this work and literature, at 353 K.

Ionic Liquid	[C ₄ mim]Cl	$[C_4 mim][MeSO_4]$	$[C_4 mim][NTf_2]$
Present Study	179.2 ± 0.0	181.0 ± 8.1	73.4 ± 2.3
Taguchi et al. ⁴⁶	228.9	_	_
Jang et al. 47	218.2^{a}	_	_
Kumelan et al. ⁴⁸	_	184.4 ± 2.5	_
Raeissi et al. ⁴⁹	_	_	67.1
Carvalho et al. ⁵⁰	_	_	$64.1 \text{ or } 54.7^b$
Jacquemin et al. ⁵¹	_	_	66.5^{b}

 $[^]ak_{H, \rm CO_2}$ calculated by taking

a linear-fit of the data ranging from 24.54 to 43.38 bar

 $^{{}^{}b}k_{H,CO_{2}}$ at 343 K

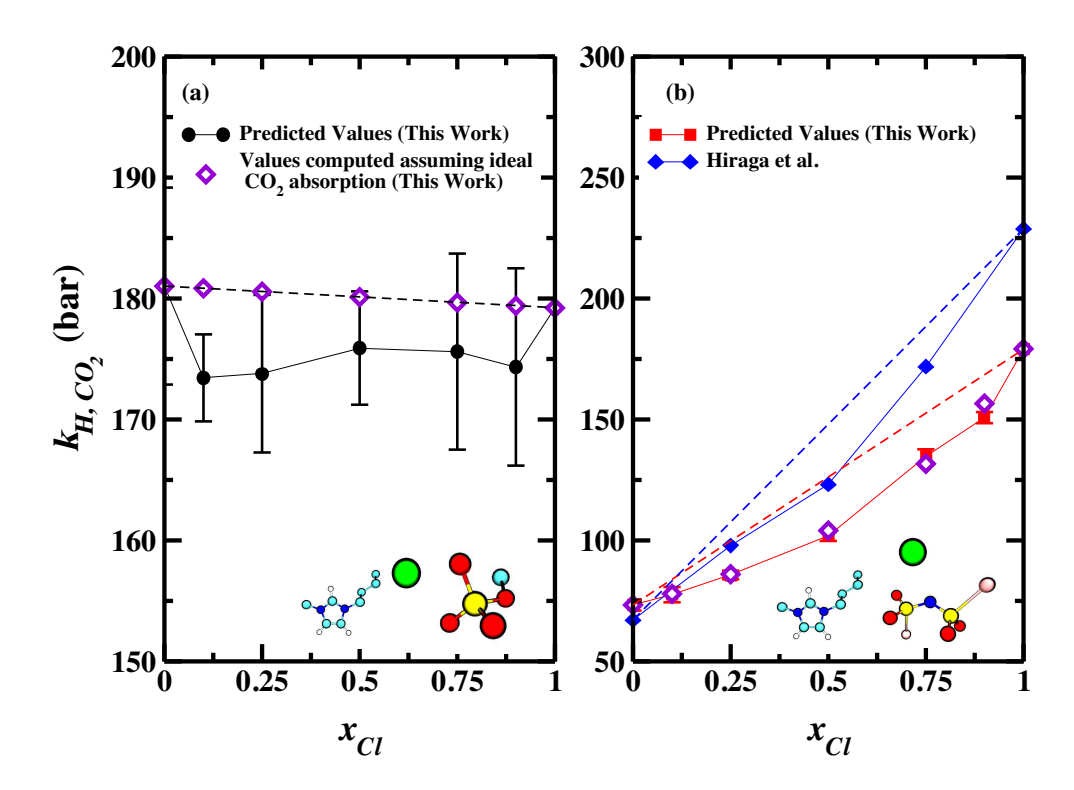


Figure 1: Comparison of Henry's constants, k_H , of CO₂ between the predicted values obtained from thermodynamic integration, values extrapolated using mole fraction weighted average harmonic mean, and available literature data (Hiraga et al. ³⁰); as a function of Cl⁻ composition in binary ionic liquid mixture of (a) $[C_4 \text{mim}] Cl_x [MeSO_4]_{1-x}$ and (b) $[C_4 \text{mim}] Cl_x [NTf_2]_{1-x}$ at 353 K. Please note that the dotted-line is shown as a reference for the linear mixing average while the solid-lines joining data points are only guide to the eye. The standard deviations were calculated from three independent molecular dynamics (MD) trials for all the mixture compositions.

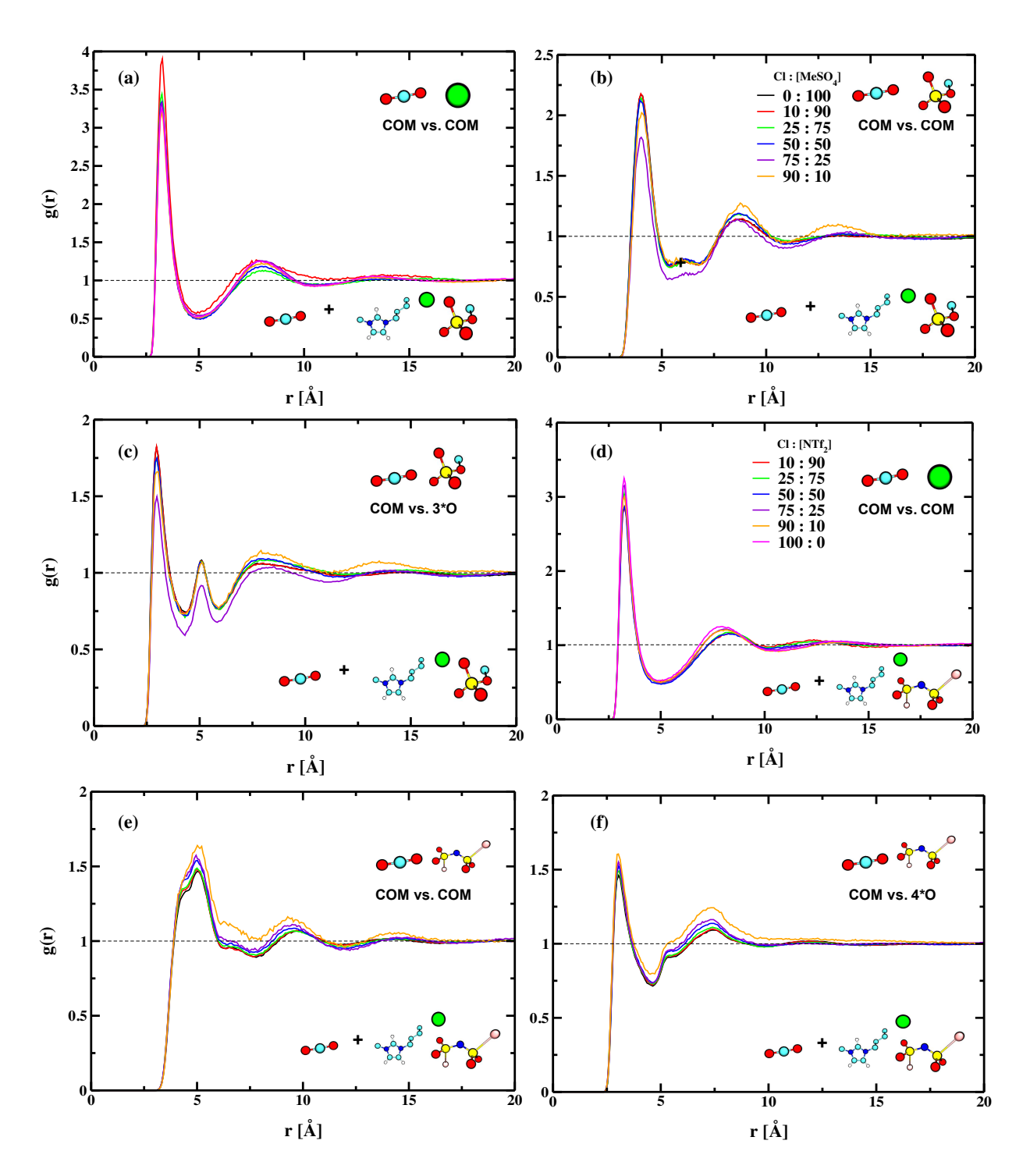


Figure 2: Radial distribution functions (RDFs) between CO_2 molecules and (a) Cl^- (b) $[MeSO_4]^-$ (c) 3 equivalent oxygen's (O) of $[MeSO_4]^-$ in $[C_4mim]Cl_x[MeSO_4]_{1-x}$. Similarly (d), (e), and (f) represents RDFs between CO_2 and Cl^- , $[NTf_2]^-$ and 4 equivalent oxygen's (O) of $[NTf_2]^-$ anion in $[C_4mim]Cl_x[NTf_2]_{1-x}$ at 353 K with varying Cl^- composition. Please refer to Figure S1 of the supporting information for the atomic nomenclature. Also note that molecules shown in top-right corner represents the molecules used to compute the RDFs, while the molecule representation at the bottom represents the simulation system of ionic liquid mixture. The COM abbreviation stands for the center-of-mass.

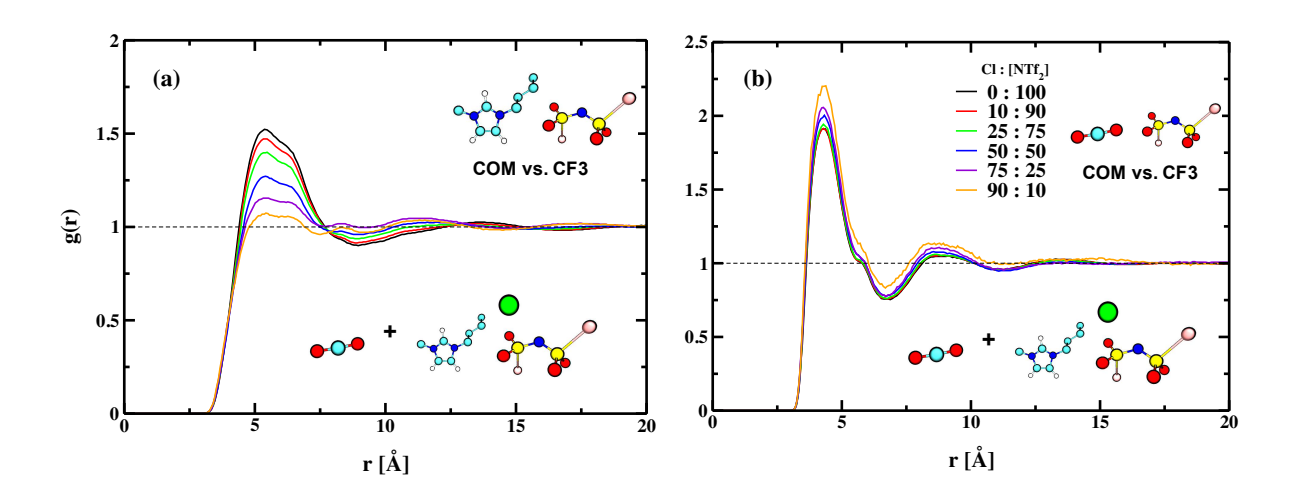


Figure 3: Radial distribution functions (RDFs) (a) between $[C_4 mim]^+$ (COM) and CF3 atom of the $[NTf_2]^-$ anion and (b) between CO_2 molecules and CF3 atom of the $[NTf_2]^-$ anion, in $[C_4 mim] Cl_x [NTf_2]_{1-x}$ at 353 K with varying Cl⁻ ion concentration. Please refer to Figure S1 of the supporting information for the atomic nomenclature. Also note that molecules shown in top-right corner represents the molecules used to compute the RDFs, while the molecule representation at the bottom represents the simulation system of ionic liquid mixture. The COM abbreviation stands for the center-of-mass.

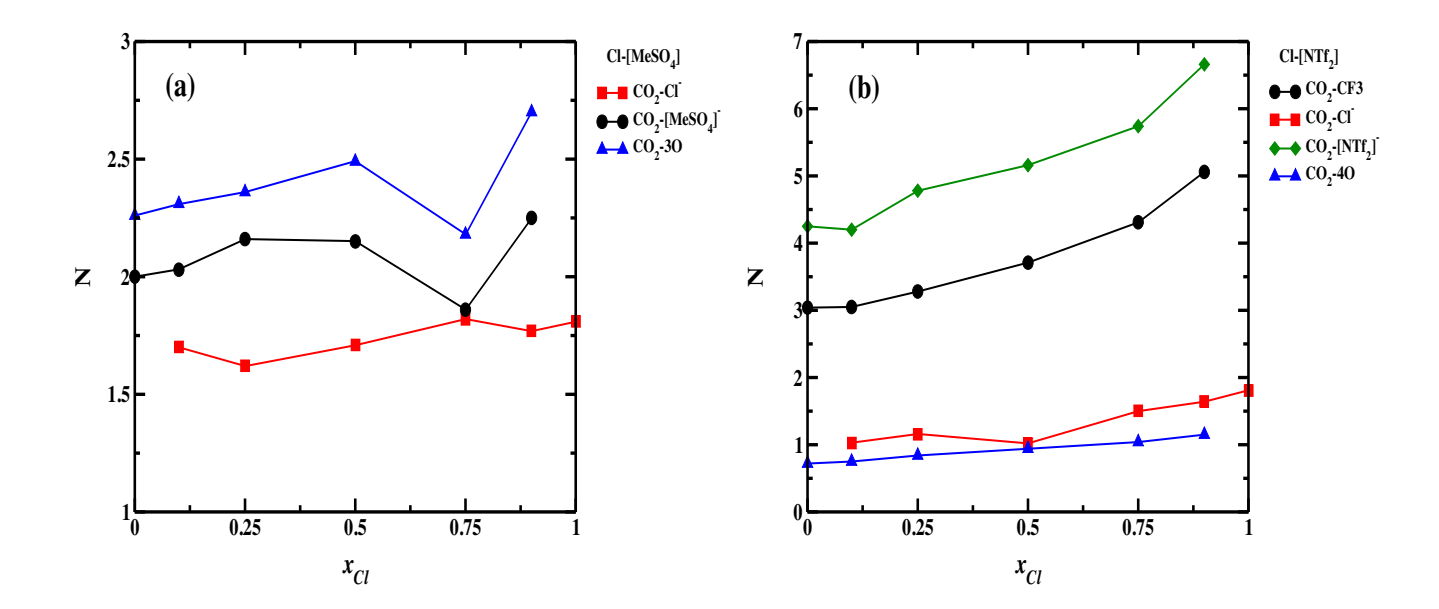


Figure 4: Average number of CO_2 molecules around both anions (Cl⁻ and [MeSO₄]⁻ on the left and Cl⁻ and [NTf₂]⁻ on the right) in the first coordination shell of an anion as a function of mixture composition at 353 K. Note that the radius of first solvation shell is determined from the respective CO_2 -anion RDFs.

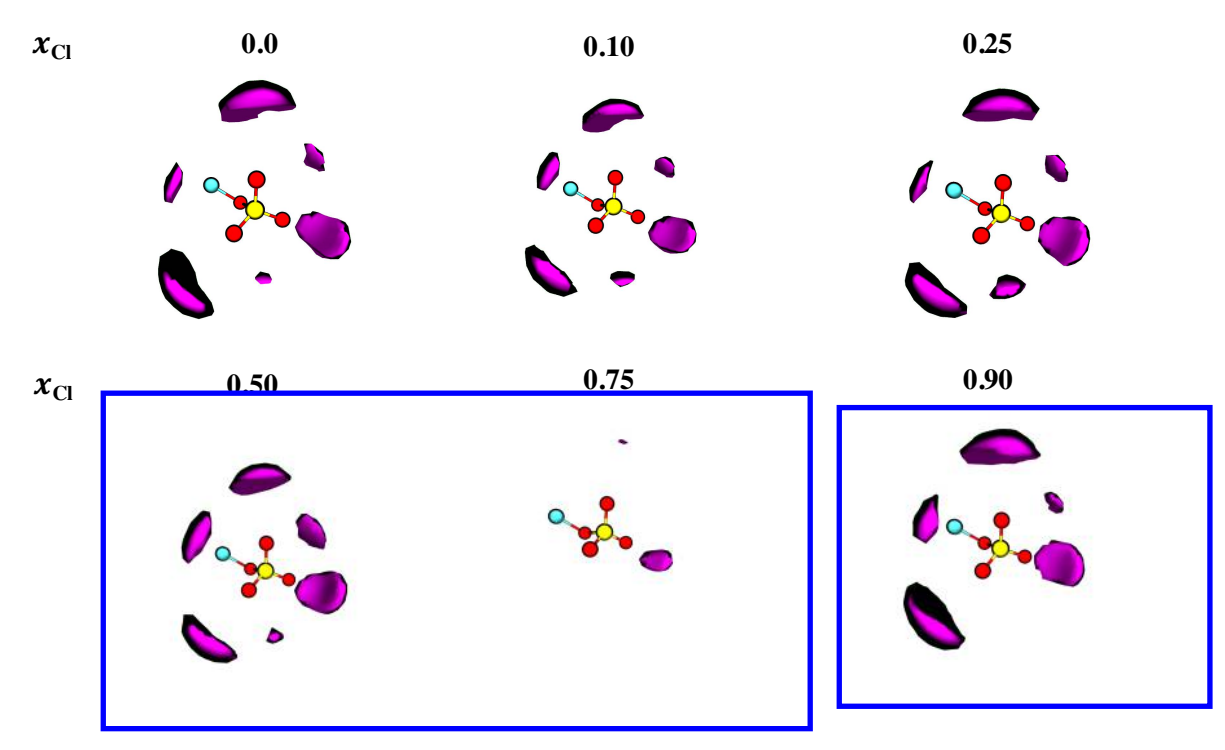


Figure 5: Spatial distribution functions (SDFs) of CO_2 molecules around the $[MeSO_4]^-$ anion in $[C_4mim]Cl_x[MeSO_4]_{1-x}$ mixture system. Isosurface density is 2.0 times the bulk density. The top row, x_{Cl} , represents the Cl^- concentration. Color coding: CO_2 in purple. Atoms: S yellow, O red and C cyan.

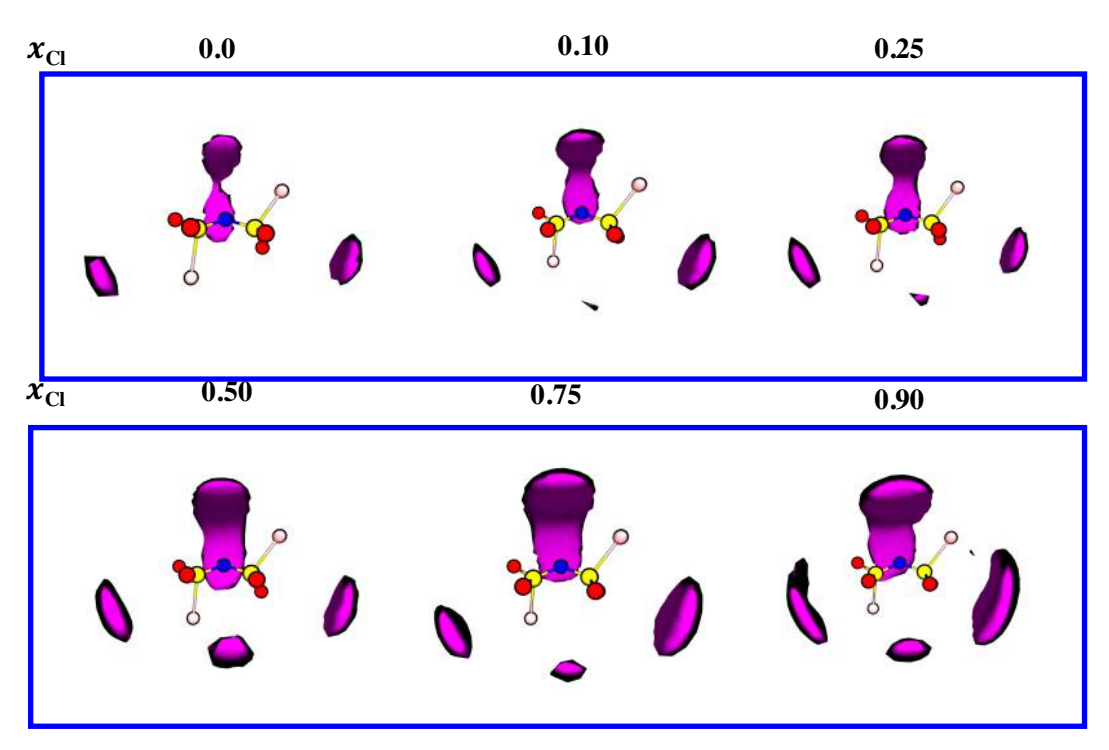


Figure 6: Spatial distribution functions (SDFs) of CO_2 molecules around the $[NTf_2]^-$ anion in $[C_4 mim] Cl_x [NTf_2]_{1-x}$ mixture system. Isosurface density is 2.0 times the bulk density. The top row, x_{Cl} , represents the Cl^- concentration. Color coding: CO_2 in purple. Atoms: S yellow, O red, N blue and CF3 orange.

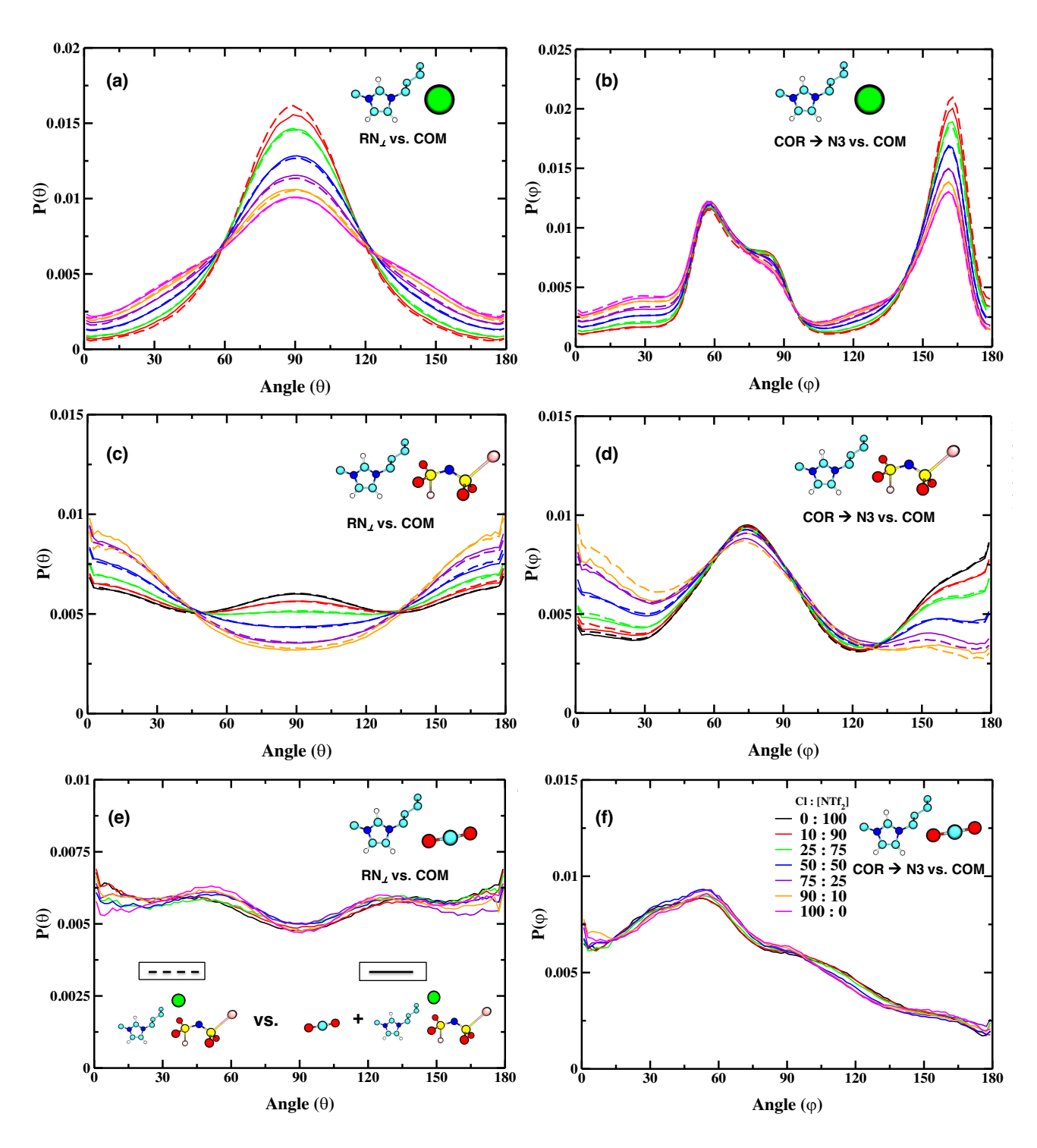
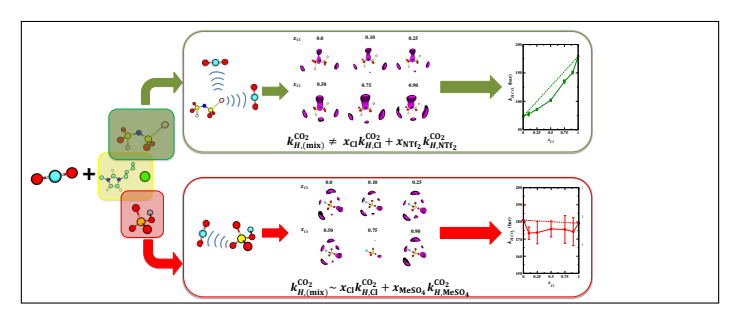


Figure 7: Angular distribution functions (ADFs) of Cl^- , $[NTf_2]^-$ anions and CO_2 molecules around $[C_4mim]^+$ within the first solvation shell, defined by the respective RDF minimum, for mixture system of $[C_4mim]Cl_x[NTf_2]_{1-x}$ are shown in (a) - (b); (c) - (d); and (e) - (f) respectively. Please note that molecules shown in top-right corner represents the molecules used to compute the ADFs, along with the vectors, while the molecule representation at the bottom represents the simulation system of ionic liquid mixture. The abbreviations used are COM for the center-of-mass, RN for ring-normal and COR for the center-of-ring. Furthermore, for direct comparison ADFs with and without CO_2 molecules in ionic liquid mixture systems are plotted together; solid-line with CO_2 while dotted-line without CO_2 molecules.

Graphical TOC Entry



Non-linearity in ${\rm CO}_2$ Henry's constants is due to enhanced interaction between CO_2 and $[NTf_2]^{-1}$ anion.

 $\ensuremath{\mathsf{CO}}_2\xspace$ -anion interactions in pure ionic liquids are retained in binary ionic liquid mixtures as well, leading to linear mixing behavior of CO₂ Henry's constants.

